

## Continuum-discretized coupled-channels method for four-body nuclear breakup in ${}^6\text{He}+{}^{12}\text{C}$ scattering

T. Matsumoto,<sup>1</sup> E. Hiyama,<sup>2</sup> K. Ogata,<sup>1</sup> Y. Iseri,<sup>3</sup> M. Kamimura,<sup>1</sup> S. Chiba,<sup>4</sup> and M. Yahiro<sup>1</sup>

<sup>1</sup>*Department of Physics, Kyushu University, Fukuoka 812-8581, Japan*

<sup>2</sup>*Department of Physics, Nara Women's University, Nara 630-8506, Japan*

<sup>3</sup>*Department of Physics, Chiba-Keizai College, Inage, Chiba 263-0021, Japan*

<sup>4</sup>*Advanced Science Research Center, Japan Atom Energy Research Institute (JAERI), Tokai, Ibaraki 319-1195, Japan*

(Received 8 September 2004; published 13 December 2004)

We propose a fully quantum-mechanical method of treating four-body nuclear breakup processes in scattering of a projectile consisting of three constituents, by extending the continuum-discretized coupled-channels method. The three-body continuum states of the projectile are discretized by diagonalizing the internal Hamiltonian of the projectile with the Gaussian basis functions. For  ${}^6\text{He}+{}^{12}\text{C}$  scattering at 18 and 229.8 MeV, the validity of the method is tested by convergence of the elastic and breakup cross sections with respect to increasing the number of the basis functions. Effects of the four-body breakup and the Borromean structure of  ${}^6\text{He}$  on the elastic and total reaction cross sections are discussed.

DOI: 10.1103/PhysRevC.70.061601

PACS number(s): 21.45.+v, 21.60.Gx, 24.10.Eq, 25.60.-t

The study on neutron-halo nuclei has become one of the central subjects in the unstable nuclear physics since the discovery of such nuclei [1]. In scattering of a two-neutron-halo nucleus such as  ${}^6\text{He}$  and  ${}^{11}\text{Li}$ , the projectile easily breaks up into its three constituents ( $n+n+\text{core}$ ), indicating that the scattering should be described as a four-body ( $n+n+\text{core}+\text{target}$ ) reaction. Then an accurate theory for treating such a four-body breakup is highly desirable.

So far the eikonal and adiabatic calculations were proposed and applied to  ${}^6\text{He}$  and  ${}^{11}\text{Li}$  scattering around 50 MeV/nucleon [2–5]. Since these calculations are based on semiclassical approaches, they work well at higher incident energies. In fact, the elastic cross section of  ${}^6\text{He}+{}^{12}\text{C}$  scattering at 229.8 MeV has recently been measured [6] and successfully analyzed by the eikonal calculation with the six-nucleon wave function of  ${}^6\text{He}$  [7]. However, these approaches seem not to be applicable for low-energy scattering such as  ${}^6\text{He}+{}^{12}\text{C}$  scattering at 18 MeV [8] measured very recently.

In this Rapid Communication, we present a fully quantum-mechanical method of treating four-body nuclear breakup. The method is constructed by extending the continuum-discretized coupled-channels method (CDCC) [9] that treats three-body breakup processes in scattering of the two-body projectile. In CDCC, the total scattering wave function is expanded in terms of bound and continuum states of the projectile. The continuum states are classified by the linear ( $k$ ) and angular momenta, and they are truncated by setting an upper limit to each quantum number. The  $k$  continuum is then divided into small bins and the continuum states in each bin are averaged into a single state. This procedure of discretization is called the average (Av) method. The  $S$ -matrix elements calculated with CDCC converge as the model space is extended [9]. The converged CDCC solution is the unperturbed solution of the distorted Faddeev equations, and corrections to the solution are negligible within the region of space in which the reaction takes place [10].

Also for four-body breakup processes in scattering of the three-body projectile, CDCC has to prepare three-body bound and discretized-continuum states of the projectile. Because of the difficulty of preparing all the three-body states with the Av method, CDCC so far analyzed  ${}^6\text{He}$  scattering within a limited model in which a two-neutron pair is treated as a single particle, di-neutron ( ${}^2n$ ) [11]. However, the accuracy of the di-neutron model has not been confirmed yet, because of the absence of fully quantum-mechanical method of treating four-body breakup.

In our previous work [12] on three-body breakup in scattering of the two-body projectile, we proposed a new method of discretization, called the pseudostate (PS) method. In the method, continuum states of the projectile are replaced by discrete pseudostates obtained by diagonalizing the internal Hamiltonian of the projectile in a space spanned by the  $L^2$ -type Gaussian basis functions. The CDCC solution calculated by the PS method agrees with that by the Av method, which can be regarded as the exact solution. Thus, a reasonable number of Gaussian basis functions can form an approximate complete set in a finite configuration space being important for three-body breakup processes. It is very likely that the approximate completeness persists also in the case of four-body breakup processes. Actually, as shown in the latter, we can see a clear convergence of calculated elastic and breakup cross sections with respect to an increasing number of Gaussian basis functions. It should be noted that the Gaussian basis functions are widely used to solve bound-state problems of few-body systems [13], since the use of the basis functions reduces numerical works much. Thus, the four-body breakup processes can be analyzed properly by CDCC with the PS method. We refer to this new method as *four-body CDCC* and the usual CDCC for three-body breakup as *three-body CDCC*.

The first application of four-body CDCC thus designed is made for  ${}^6\text{He}+{}^{12}\text{C}$  scattering at 18 and 229.8 MeV, where the projectile has the Borromean structure and then easily breaks up into two nucleons and  ${}^4\text{He}$ . In these scattering

processes, the incident energies  $E_{\text{in}}$  are much higher than the Coulomb barrier energy ( $\sim 3$  MeV), so only nuclear breakup processes become significant. We thus concentrate our application on nuclear breakup. The calculated elastic cross sections well reproduce experimental data at both  $E_{\text{in}}$ . Moreover, effects of the four-body breakup and the Borromean structure of  ${}^6\text{He}$  on the elastic and total reaction cross sections are discussed in the case of  $E_{\text{in}}=18$  MeV.

We assume that  ${}^6\text{He}+{}^{12}\text{C}$  scattering is described as a four-body system,  $n+n+{}^4\text{He}+{}^{12}\text{C}$ . Then, the Schrödinger equation can be written as

$$\left[ K_R + \sum_{i \in \text{P}} \sum_{j \in \text{T}} v_{ij} + V_C(R) + H_6 - E \right] \Psi(\xi, \mathbf{R}) = 0, \quad (1)$$

where  $\mathbf{R}$  and  $\xi$  are, respectively, the coordinate of the center of mass of  ${}^6\text{He}$  relative to  ${}^{12}\text{C}$  and the internal coordinates of  ${}^6\text{He}$ ;  $K_R$  is the kinetic energy associated with  $\mathbf{R}$ . Here,  $H_6$  is the internal Hamiltonian of the  ${}^6\text{He}$  projectile, and  $E$  is the sum of  $E_{\text{in}}$  and the ground state energy of  ${}^6\text{He}$ . The  $v_{ij}$  represent two-body nuclear interactions working between the  ${}^6\text{He}$  projectile (P) and the  ${}^{12}\text{C}$  target (T). Meanwhile, the Coulomb potential  $V_C$  is treated approximately as a function of  $R$  only, i.e., we neglect Coulomb breakup processes.

The four-body wave function  $\Psi^{JM}$ , where  $J$  is the total angular momentum of the four-body system and  $M$  is its projection on the  $z$  axis, is expanded in terms of a finite number of the internal wave functions  $\Phi_{nlm}$  of the  ${}^6\text{He}$  projectile,

$$\Psi^{JM}(\xi, \mathbf{R}) = \sum_{nL} \chi_{nL}^J(P_{nl}, R) / R \mathcal{Y}_{nL}^{JM}, \quad (2)$$

where  $\mathcal{Y}_{nL}^{JM} = [\Phi_{nl}(\xi) \otimes i^L Y_L(\hat{\mathbf{R}})]_{JM}$ . Here  $I$  is the total spin of  ${}^6\text{He}$  and  $m$  is its projection on the  $z$  axis, and  $n$  stands for the  $n$ th eigenstate. The  $\Phi_{nlm}$  satisfies  $H_6 \Phi_{nlm} = \epsilon_{nl} \Phi_{nlm}$  and the expansion coefficient  $\chi_{nL}^J$  in Eq. (1) represents the relative motion between the projectile and the target;  $L$  is the orbital angular momentum regarding  $\mathbf{R}$ . The relative momentum  $P_{nl}$  is determined by the conservation of the total energy:  $E = P_{nl}^2 / 2\mu + \epsilon_{nl}$ , with  $\mu$  the reduced mass between the projectile and the target. Multiplying Eq. (1) by  $\mathcal{Y}_{n'L}^{*JM}$  from the left, one can obtain a set of coupled differential equations for  $\chi_{nL}^J$ , called the CDCC equation; it should be noted that the CDCC equation for the four-body system is formally equal to that for the three-body system. Solving the CDCC equation under the appropriate asymptotic boundary condition [9,14], we can obtain the elastic and discrete breakup  $S$ -matrix elements. Details of the formalism of CDCC are shown in Ref. [9].

In the Gaussian expansion method [13],  $\Phi_{nlm}$  is written as

$$\Phi_{nlm}(\xi) = \sum_{c=1}^3 \psi_{nlm}^{(c)}(\xi), \quad (3)$$

where  $c$  denotes a set of Jacobian coordinates in Fig. 1. Each  $\psi_{nlm}^{(c)}$  is expanded in terms of the Gaussian basis functions

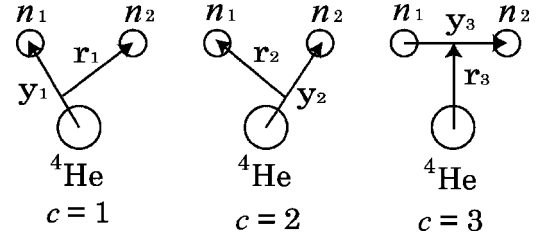


FIG. 1. Jacobian coordinates of three rearrangement channels ( $c=1-3$ ) adopted for the  $n+n+{}^4\text{He}$  model of  ${}^6\text{He}$  structure.

$$\psi_{nlm}^{(c)}(\xi) = \varphi^{(\alpha)} \sum_{\lambda \ell \Lambda S} A_{i\lambda j \ell \Lambda S}^{(c)nl} \mathcal{Y}_c^\lambda r_c^\ell e^{-(y_c/\bar{y}_i)^2} e^{-(r_c/\bar{r}_j)^2} \times [[Y_\lambda(\hat{y}_c) \otimes Y_\ell(\hat{r}_c)]_\Lambda \otimes [\eta_{1/2}^{(n_1)} \otimes \eta_{1/2}^{(n_2)}]_S]_{lm}, \quad (4)$$

where  $\lambda$  ( $\ell$ ) is the angular momentum regarding the Jacobian coordinates  $\mathbf{y}_c$  ( $\mathbf{r}_c$ ), and  $\eta_{1/2}$  is the spin wave function of each valence neutron ( $n_1$  or  $n_2$ ).  ${}^4\text{He}$  has been treated as an inert core with the  $(0s)^4$  internal configuration,  $\varphi^{(\alpha)}$ . The Gaussian range parameters are taken to lie in geometric progression

$$\bar{y}_i = \bar{y}_1 (\bar{y}_{\text{max}} / \bar{y}_1)^{(i-1)/(i_{\text{max}}-1)}, \quad (5)$$

$$\bar{r}_j = \bar{r}_1 (\bar{r}_{\text{max}} / \bar{r}_1)^{(j-1)/(j_{\text{max}}-1)}. \quad (6)$$

$\Phi_{nlm}$  is antisymmetrized for the exchange between  $n_1$  and  $n_2$ ; we then have  $A_{i\lambda j \ell \Lambda S}^{(2)nl} = (-)^S A_{i\lambda j \ell \Lambda S}^{(1)nl}$ , and  $(-)^{\lambda+S} = 1$  for  $c=3$ . Meanwhile, the exchange between each valence neutron and each nucleon in  ${}^4\text{He}$  is treated approximately by the orthogonality condition model [15]. The eigenenergies  $\epsilon_{nl}$  of  ${}^6\text{He}$  and the corresponding expansion coefficients  $A_{i\lambda j \ell \Lambda S}^{(c)nl}$  are determined by diagonalizing  $H_6$  [16,17].

In the four-body CDCC calculation shown below, we take  $I^\pi=0^+$  and  $2^+$  states for  ${}^6\text{He}$ . Here we omit the  $1^-$  and  $3^-$  states that do not contribute to the nuclear breakup processes. The calculated  $\epsilon_{nl}$  are  $-0.98$  MeV for the  $0^+$  ground state and  $0.72$  MeV for the  $2^+$  resonance state, which well reproduce the corresponding experimental values. We show in Table I the maximum values of the internal angular momenta,  $\lambda_{\text{max}}$ ,  $\ell_{\text{max}}$ , and  $\Lambda_{\text{max}}$ , and the Gaussian range parameters,  $\bar{y}_1$ ,  $\bar{y}_{\text{max}}$ ,  $\bar{r}_1$ , and  $\bar{r}_{\text{max}}$ , used in the calculation of  $\Phi_{nlm}$ . It should be noted that most of them depend on  $I^\pi$  and  $c$ , while in Eqs. (4)–(6) the dependence has been omitted for simplicity.

In order to demonstrate the convergence of the four-body CDCC solution with an increasing number of Gaussian basis functions, we prepare three sets of the basis functions, i.e., sets I, II, and III. Each set is specified by  $i_{\text{max}}^{I^\pi(c)}$  and  $j_{\text{max}}^{I^\pi(c)}$ . One can calculate the total number of the eigenenergies of  $H_6$ ,  $\mathcal{N}_{\text{max}}^{I^\pi}$ , by using Eqs. (3)–(6) and the input parameters shown in Table I. The values of  $i_{\text{max}}^{I^\pi(c)}$ ,  $j_{\text{max}}^{I^\pi(c)}$ , and  $\mathcal{N}_{\text{max}}^{I^\pi}$  for each set are shown in Table II. In the actual CDCC calculation for  ${}^6\text{He}+{}^{12}\text{C}$  scattering at 18 MeV (229.8 MeV), high-lying states with  $\epsilon_{nl} > 12$  MeV ( $\epsilon_{nl} > 25$  MeV) are found to give no effect on the elastic and breakup  $S$ -matrix elements. Thus,

TABLE I. The maximum internal angular momenta and the Gaussian range parameters for each Jacobian coordinate.

$c$	$I^\pi$	$\lambda_{\max}$	$\ell_{\max}$	$\Lambda_{\max}$	$\bar{y}_1$ (fm)	$\bar{y}_{\max}$ (fm)	$\bar{r}_1$ (fm)	$\bar{r}_{\max}$ (fm)
3	$0^+$	1	1	1	0.1	10.0	0.5	10.0
1,2	$0^+$	1	1	1	0.5	10.0	0.5	10.0
3	$2^+$	2	2	2	0.5	10.0	0.5	8.0
1,2	$2^+$	1	1	2	0.5	10.0	0.5	8.0

the effective number of the eigenstates of  ${}^6\text{He}$ ,  $N_{\max}^{j^\pi}$ , is reduced much for each of sets I–III, as shown in Table II.

As for the coupling potentials in the CDCC equation, we adopt the double-folding model [18] as follows:

$$U_{\zeta'\zeta}^J(R) = (N_R + iN_I)V_{\zeta'\zeta}^J(R), \quad (7)$$

$$V_{\zeta'\zeta}^J(R) \equiv \langle \mathcal{Y}_{n'l'l',L}^{JM} | \Phi_{\text{g.s.}}^{(T)} | \sum_{i \in \text{P}} \sum_{j \in \text{T}} v_{ij} | \Phi_{\text{g.s.}}^{(T)} | \mathcal{Y}_{n'l,L}^{JM} \rangle$$

$$= \int \rho_{\zeta'\zeta}^{(P)JM}(\mathbf{r}_P, \hat{\mathbf{R}}) \rho_{\text{g.s.}}^{(T)}(\mathbf{r}_T) v_{\text{NN}}(E, \rho, \mathbf{s}) d\mathbf{r}_T d\mathbf{r}_P d\hat{\mathbf{R}}, \quad (8)$$

where  $\mathbf{r}_P$  ( $\mathbf{r}_T$ ) is the coordinate of a nucleon in the projectile (target) relative to the center of mass of the particle, and  $\mathbf{s} = \mathbf{R} + \mathbf{r}_T - \mathbf{r}_P$ . The quantum number  $\zeta$  represents  $\zeta = (n, l, L)$ , and the elastic channel is denoted by  $\zeta_0 \equiv (0, l_0, L_0)$  with  $l_0 = 0$  and  $L_0 = J$ . The ground state density of  ${}^{12}\text{C}$ ,  $\rho_{\text{g.s.}}^{(T)}(\mathbf{r}_T) \equiv \langle \Phi_{\text{g.s.}}^{(T)} | \sum_{j=1}^{12} \delta(\mathbf{r}_T - \mathbf{r}_j) | \Phi_{\text{g.s.}}^{(T)} \rangle$ , where  $\Phi_{\text{g.s.}}^{(T)}$  is the wave function of  ${}^{12}\text{C}$  in the ground state, is calculated by the microscopic  $3\alpha$  cluster model [19]. In this study, we define the transition densities of  ${}^6\text{He}$ ,  $\rho_{\zeta'\zeta}^{(P)JM}$ , as

$$\rho_{\zeta'\zeta}^{(P)JM}(\mathbf{r}_P, \hat{\mathbf{R}}) = \langle \mathcal{Y}_{n'l'l',L}^{JM} | \sum_{i=1}^6 \delta(\mathbf{r}_P - \mathbf{r}_i) | \mathcal{Y}_{n'l,L}^{JM} \rangle_{\zeta}. \quad (9)$$

As for the nucleon-nucleon effective interaction  $v_{\text{NN}}$ , we use the realistic energy- and density-dependent M3Y (DDM3Y) interaction [20]. Since the DDM3Y interaction is real,  $V_{\zeta'\zeta}^J$  has no imaginary part. Thus, we have multiplied  $V_{\zeta'\zeta}^J$  by a complex factor  $N_R + iN_I$ . In the present analysis, we fix  $N_R = 1$  and optimize  $N_I$  to fit experimental data for elastic scattering. It should be noted that in the three-body CDCC calculation made before for  ${}^6\text{Li}$  scattering on various target nu-

clei [21,22], the prescription above was successful in reproducing experimental data.

The convergence of the four-body CDCC solution is tested for  ${}^6\text{He} + {}^{12}\text{C}$  scattering at 18 MeV. Figure 2 shows the energy-integrated breakup cross section, i.e., the sum of the cross sections to all breakup channels, calculated with sets I–III. The results of sets II and III are in good agreement with each other, but the result of set I is somewhat different from them. Meanwhile, as for the elastic cross section shown in Fig. 3, the three sets give the same cross section, which is shown by the solid line. Thus, the four-body CDCC solution converges with set II. Furthermore, we have confirmed that similar convergence is also seen with respect to extending  $\bar{y}_{\max}$  and  $\bar{r}_{\max}$ . The optimum value of  $N_I$  determined from the measured elastic cross section is 0.5 at  $E_{\text{in}} = 18$  MeV, which is the same as that for  ${}^6\text{Li}$  scattering at various  $E_{\text{in}}$  [21,22]. It should be noted that all calculations shown in Figs. 2 and 3 use the same value of  $N_I$ . Also for  ${}^6\text{He} + {}^{12}\text{C}$  scattering at 229.8 MeV, we can see a similar convergence of the elastic and energy-integrated breakup cross sections with respect to extending the model space. Comparison between the calculated and measured elastic cross sections is shown in Fig. 4. In this case the optimum value of  $N_I$  is 0.3. In Figs. 3 and 4, the dotted lines represent the elastic cross sections due to the single-channel calculation. Then, the difference between the solid and dotted lines shows the effect of the four-body breakup on the elastic cross section. For both  $E_{\text{in}}$ , the effect is sizable, the properties of which are discussed later.

Recently, it was reported in Ref. [11] that the total reaction cross section for  ${}^6\text{He} + {}^{209}\text{Bi}$  is much larger than that for  ${}^6\text{Li} + {}^{209}\text{Bi}$  at similar energies relative to the Coulomb barrier energies because of the large  $E1$  excitation strength of  ${}^6\text{He}$  to the continuum. Meanwhile, for  ${}^6\text{He} + {}^{12}\text{C}$  scattering at 18 MeV, the  $E1$  excitation of  ${}^6\text{He}$  is negligible because  $E_{\text{in}}$  is much higher than the Coulomb barrier energy (about 3 MeV). As shown in Fig. 5, however, we find that 15% enhancement of the total reaction cross section is still left. The open circles represent the total reaction cross sections for  ${}^6\text{He} + {}^{12}\text{C}$  at 18 and 229.8 MeV, calculated by four-body CDCC, while the filled circles show those for  ${}^6\text{Li} + {}^{12}\text{C}$  in the energy range 20–318 MeV, calculated by three-body CDCC [21,22], where the microscopic  $d + {}^4\text{He}$  model is assumed for the  ${}^6\text{Li}$  structure. As mentioned above, the resulting optimum  $N_I$  value for  ${}^6\text{Li} + {}^{12}\text{C}$  is about 0.5, i.e., almost independent of  $E_{\text{in}}$ .

In order to investigate the origin of the 15% enhancement, we perform the three-body CDCC calculation by assuming the di-neutron model for  ${}^6\text{He}$  structure; in the model, the

TABLE II. The number of the Gaussian basis functions,  $i_{\max}^{j^\pi(c)}$  and  $j_{\max}^{j^\pi(c)}$  for sets I, II, and III. The corresponding number of eigenstates of  $H_6$ ,  $\mathcal{N}_{\max}^{j^\pi}$ , and the number of channels included in the CDCC equation,  $N_{\max}^{j^\pi}$ , are also shown (see the text for the details).

	$i_{\max}^{0^+(3)}$	$j_{\max}^{0^+(3)}$	$i_{\max}^{0^+(1,2)}$	$j_{\max}^{0^+(1,2)}$	$\mathcal{N}_{\max}^{0^+}$	$i_{\max}^{2^+(1,2,3)}$	$j_{\max}^{2^+(1,2,3)}$	$\mathcal{N}_{\max}^{2^+}$	18 MeV $\mathcal{N}_{\max}^{0^+}$	18 MeV $\mathcal{N}_{\max}^{2^+}$	229.8 MeV $\mathcal{N}_{\max}^{0^+}$	229.8 MeV $\mathcal{N}_{\max}^{2^+}$
Set I	8	6	6	6	204	6	6	288	17	21	28	39
Set II	10	8	8	8	352	8	8	512	25	32	44	64
Set III	12	10	10	10	540	10	10	800	32	42	60	85

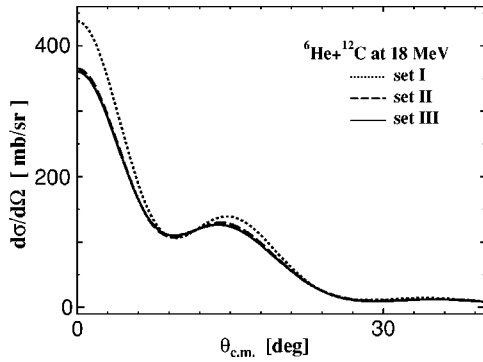


FIG. 2. Angular distribution of the energy-integrated breakup cross section for  ${}^6\text{He}+{}^{12}\text{C}$  scattering at 18 MeV. The dotted, dashed, and solid lines are the results of the four-body CDCC calculation with sets I, II, and III, respectively, of the Gaussian basis functions.

di-neutron density is assumed to be the same as that of the deuteron, and then the resulting  ${}^6\text{He}$  density is close to the  ${}^6\text{Li}$  one. The result of this calculation is shown by the open triangle in Fig. 5. The difference between the open triangle and the open circle at 18 MeV is due to the Borromean structure of  ${}^6\text{He}$ , which is referred to as the Borromean effect. The effect dominates about half the 15% enhancement. The rest of the enhancement is mainly due to the difference of the Coulomb barrier energies between  ${}^6\text{He}+{}^{12}\text{C}$  and  ${}^6\text{Li}+{}^{12}\text{C}$ . Actually, when the Coulomb potential for  ${}^6\text{He}+{}^{12}\text{C}$  is replaced artificially by that for  ${}^6\text{Li}+{}^{12}\text{C}$ , the CDCC calculation based on the di-neutron model (the filled triangle) gives the total reaction cross section close to the filled circle at 20 MeV.

As for  ${}^6\text{He}+{}^{12}\text{C}$  scattering at 229.8 MeV, we have confirmed through the same analysis that the Borromean effect becomes negligible, as well as the effect of the difference of the Coulomb barrier between  ${}^6\text{He}+{}^{12}\text{C}$  and  ${}^6\text{Li}+{}^{12}\text{C}$ . This suggests no enhancement theoretically. Nevertheless, Fig. 5 shows that the total reaction cross section for  ${}^6\text{He}+{}^{12}\text{C}$  is even smaller than that for  ${}^6\text{Li}+{}^{12}\text{C}$  at a similar energy. This curious behavior is due to the fact that  $N_I=0.3$  for  ${}^6\text{He}+{}^{12}\text{C}$  while  $N_I=0.5$  for  ${}^6\text{Li}+{}^{12}\text{C}$  at this high energy. In fact, the total reaction cross section is enhanced by changing  $N_I$

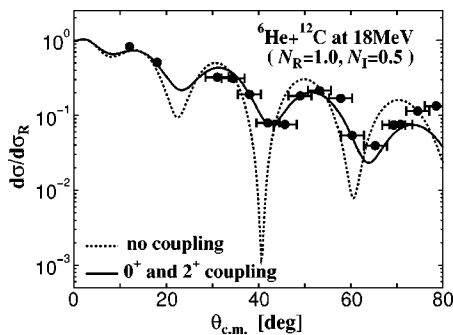


FIG. 3. Angular distribution of the elastic differential cross section for  ${}^6\text{He}+{}^{12}\text{C}$  scattering at 18 MeV. The solid and dotted lines show the results with and without breakup effects, respectively. The experimental data are taken from Ref. [8].

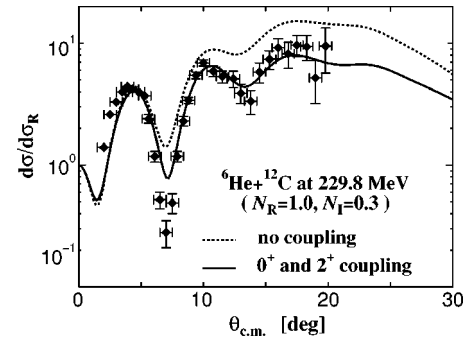


FIG. 4. The same as in Fig. 3 but for  ${}^6\text{He}+{}^{12}\text{C}$  scattering at 229.8 MeV. The experimental data are taken from Ref. [6].

from 0.3 to 0.5 in four-body CDCC calculation for  ${}^6\text{He}+{}^{12}\text{C}$ , and the resulting cross section almost reproduces the corresponding one for  ${}^6\text{Li}+{}^{12}\text{C}$ . The origin of the small  $N_I$  value for the  ${}^6\text{He}$  scattering is not clear at this moment, so more systematic experimental data are highly desirable for  ${}^6\text{He}$  scattering.

Finally, we calculate the dynamical polarization (DP) potential induced by the four-body breakup processes, in order to understand effects of the processes on the elastic scattering. The DP potential  $U_{\text{DP}}^J$  is given by

$$U_{\text{DP}}^J(R) = U_{\text{eq}}^J(R) - U_{\zeta_0\zeta_0}^J(R), \quad (10)$$

where  $U_{\text{eq}}^J$  is the so-called wave-function-equivalent local potential derived using the elastic channel amplitude  $\chi_{0I_0L_0}^J$  in the solution of the CDCC equation, and  $U_{\zeta_0\zeta_0}^J$  is the double-folding potential for the elastic channel. The detailed definition of the DP potential is shown in Ref. [21]. Figure 6 shows the DP potential for the  ${}^6\text{He}+{}^{12}\text{C}$  scattering at 18 MeV with the total grazing angular momentum  $J_{\text{gr}}=10$ .

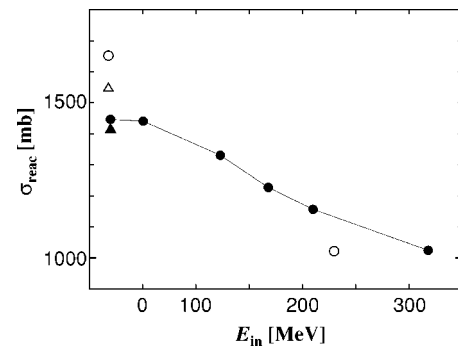


FIG. 5. The incident-energy dependence of the total reaction cross section for scattering of  ${}^6\text{He}$  and  ${}^6\text{Li}$  on  ${}^{12}\text{C}$ . The open circles show the results for  ${}^6\text{He}+{}^{12}\text{C}$  at 18 and 229.8 MeV calculated by four-body CDCC, while the filled circles represent those for  ${}^6\text{Li}+{}^{12}\text{C}$  at several energies calculated by three-body CDCC based on the  $d+{}^4\text{He}$  model for the  ${}^6\text{Li}$  structure. The open triangle is the result for  ${}^6\text{He}+{}^{12}\text{C}$  at 18 MeV calculated by three-body CDCC with the di-neutron model for the  ${}^6\text{He}$  structure. The filled triangle is based on the same calculation as the open triangle, except that the Coulomb potential between  ${}^6\text{He}$  and  ${}^{12}\text{C}$  is replaced artificially by that between  ${}^6\text{Li}$  and  ${}^{12}\text{C}$ .

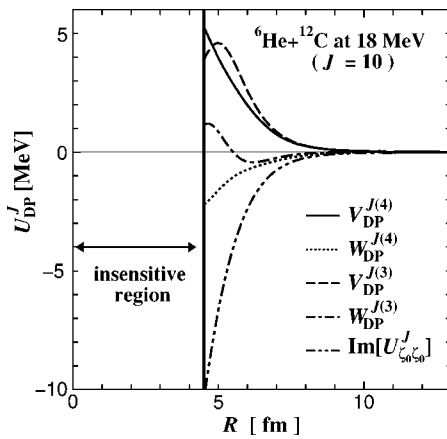


FIG. 6. The dynamical polarization potential for  ${}^6\text{He}+{}^{12}\text{C}$  scattering at 18 MeV with  $J=10$ . The solid and dotted lines, respectively, represent the real and imaginary parts of the DP potential calculated by four-body CDCC. The dashed and dot-dashed lines correspond to those of three-body CDCC with the di-neutron model for  ${}^6\text{He}$  structure. The dot-dot-dashed line represents the imaginary part of  $U_{\xi_0\xi_0}^J$ .

The “insensitive region” of  $R$  shown in the figure is defined with the condition that  $|\chi_{0l_0l_0}^J|$  is less than 5% of its maximum value in the asymptotic region. The DP potential is almost independent of  $J$  around  $J_{\text{gr}}$  in the peripheral region. In Fig. 6 the real part  $V_{\text{DP}}^{J(4)}$  ( $V_{\text{DP}}^{J(3)}$ ) and the imaginary part  $W_{\text{DP}}^{J(4)}$  ( $W_{\text{DP}}^{J(3)}$ ) of  $U_{\text{DP}}^J$  calculated by four-body (three-body) CDCC are, respectively, shown by the solid (dashed) and the dotted (dot-dashed) lines. Both of  $V_{\text{DP}}^{J(4)}$  and  $V_{\text{DP}}^{J(3)}$  are repulsive and have almost the same strength which is about 30% of the real part of  $U_{\xi_0\xi_0}^J$ . The  $W_{\text{DP}}^{J(4)}$  is about 20% of the imaginary part of  $U_{\xi_0\xi_0}^J$  (dot-dot-dashed line), while  $W_{\text{DP}}^{J(3)}$  oscillates

with  $R$ , so the net effect of  $W_{\text{DP}}^{J(3)}$  is negligibly small. Thus, one sees that inclusion of the four-body breakup processes makes the real part of the  ${}^6\text{He}-{}^{12}\text{C}$  potential shallower and the imaginary one deeper compared with  $U_{\xi_0\xi_0}^J$ . In particular, the latter effect is important and can be assumed to come from the Borromean structure of  ${}^6\text{He}$ . This is consistent with the fact that the total reaction cross section is enhanced by the Borromean structure.

In conclusion, a fully quantum-mechanical method of treating four-body nuclear breakup is presented by extending CDCC. The validity of the method called four-body CDCC is confirmed by clear convergence of the calculated elastic and energy-integrated breakup cross sections with respect to extending the modelspace. The four-body CDCC is found to explain well the  ${}^6\text{He}+{}^{12}\text{C}$  scattering at 18 and 229.8 MeV in which  ${}^6\text{He}$  easily breaks up into two neutrons and  ${}^4\text{He}$ . We find a 15% enhancement of the total reaction cross section of  ${}^6\text{He}+{}^{12}\text{C}$  at 18 MeV relative to that of  ${}^6\text{Li}+{}^{12}\text{C}$  at the similar energy. Half of the 15% enhancement is due to the Borromean structure of  ${}^6\text{He}$ . For the elastic scattering, the four-body breakup processes make, in particular, the imaginary part of the  ${}^6\text{He}-{}^{12}\text{C}$  potential deeper, which is originated in the Borromean structure of  ${}^6\text{He}$ . In the present analysis, four-body Coulomb breakup is neglected. However, it would be possible to treat the Coulomb breakup within the present framework, if the complex-range Gaussian basis functions are taken [23]. Further work along this line is highly expected.

The authors would like to thank Y. Sakuragi and M. Kawai for helpful discussions. This work has been supported in part by the Grants-in-Aid for Scientific Research (12047233, 14540271) of Monbukagakusyou of Japan. Numerical calculations were performed on FUJITSU VPP5000 at JAERI.

- 
- [1] I. Tanihata *et al.*, Phys. Lett. **160B**, 380 (1985).  
 [2] N. C. Summers *et al.*, Phys. Rev. C **66**, 014614 (2002).  
 [3] J. A. Christley *et al.*, Nucl. Phys. **A624**, 275 (1997).  
 [4] J. S. Al-Khalili *et al.*, Nucl. Phys. **A581**, 331 (1995).  
 [5] J. S. Al-Khalili *et al.*, Phys. Lett. B **378**, 45 (1996).  
 [6] V. Lapoux *et al.*, Phys. Rev. C **66**, 034608 (2002).  
 [7] B. Abu-Ibrahim and Y. Suzuki, Phys. Rev. C **70**, 011603 (2004).  
 [8] M. Milin *et al.*, Nucl. Phys. **A730**, 285 (2004).  
 [9] M. Kamimura *et al.*, Prog. Theor. Phys. Suppl. **89**, 1 (1986).  
 [10] N. Austern *et al.*, Phys. Rev. Lett. **63**, 2649 (1989); Phys. Rev. C **53**, 314 (1996).  
 [11] N. Keeley *et al.*, Phys. Rev. C **68**, 054601 (2003).  
 [12] T. Matsumoto *et al.*, Phys. Rev. C **68**, 064607 (2003).  
 [13] For a review, E. Hiyama *et al.*, Prog. Part. Nucl. Phys. **51**, 223 (2003).  
 [14] R. A. D. Piyadasa *et al.*, Phys. Rev. C **60**, 044611 (1999).  
 [15] S. Saito, Prog. Theor. Phys. **41**, 705 (1969).  
 [16] S. Funada *et al.*, Nucl. Phys. **A575**, 93 (1994).  
 [17] E. Hiyama and M. Kamimura, Nucl. Phys. **A588**, 35 (1995).  
 [18] G. R. Satchler and W. G. Love, Phys. Rep. **55**, 183 (1979).  
 [19] M. Kamimura, Nucl. Phys. **A351**, 456 (1981).  
 [20] A. M. Kobos *et al.*, Nucl. Phys. **A384**, 65 (1982).  
 [21] Y. Sakuragi *et al.*, Prog. Theor. Phys. Suppl. **89**, 136 (1986); Y. Sakuragi, Phys. Rev. C **35**, 2161 (1987).  
 [22] C. Samanta *et al.*, J. Phys. G **23**, 1697 (1997).  
 [23] T. Egami *et al.*, Phys. Rev. C **70**, 047604 (2004).